A Statistical Analysis of High-Frequency Track and Intensity Forecasts from NOAA's Operational Hurricane Weather Research and Forecasting (HWRF) Modeling System

ZHAN ZHANG,[a] JUN A. ZHANG,[b,c] GHASSAN J. ALAKA JR.,[b] KEQIN WU,[a,d] AVICHAL MEHRA,[a] AND VIJAY TALLAPRAGADA[a]

[a] *NOAA/NWS/NCEP/Environmental Modeling Center, College Park, Maryland*
[b] *NOAA/AOML/Hurricane Research Division, Miami, Florida*
[c] *Cooperative Institute for Marine and Atmospheric Studies, University of Miami, Miami, Florida*
[d] *I.M. System Group, Rockville, Maryland*

(Manuscript received 9 February 2021, in final form 15 July 2021)

ABSTRACT: A statistical analysis is performed on the high-frequency ($3^1/_3$ s) output from NOAA's cloud-permitting, high-resolution operational Hurricane Weather Research and Forecasting (HWRF) Model for all tropical cyclones (TCs) in the North Atlantic Ocean basin over a 3-yr period (2017–19). High-frequency HWRF forecasts of TC track and 10-m maximum wind speed (Vmax) exhibited large fluctuations that were not captured by traditional low-frequency (6 h) model output. Track fluctuations were inversely proportional to Vmax, with average values of 6–8 km. The Vmax fluctuations were as high as 20 kt (10.3 m s^{-1}) in individual forecasts and were a function of maximum intensity, with a standard deviation of 5.5 kt (2.8 m s^{-1}) for category-2 hurricanes and smaller fluctuations for tropical storms and major hurricanes. The radius of Vmax contracted or remained steady when TCs rapidly intensified in high-frequency HWRF forecasts, consistent with observations. Running-mean windows of 3–9 h were applied at synoptic times to smooth the high-frequency HWRF output to investigate its utility to operational forecasting. Smoothed high-frequency HWRF output improved Vmax forecast skill by up to 8% and produced a more realistic distribution of 6-h intensity change when compared with low-frequency, instantaneous output. Furthermore, the high-frequency track forecast output may be useful for investigating characteristics of TC trochoidal motions.

KEYWORDS: Tropical cyclones; Model errors; Model output statistics

1. Introduction

Although numerical weather prediction (NWP) models for tropical cyclone (TC) forecasting have become more sophisticated with high-resolution, cloud-permitting grids and advanced model physics (Gopalakrishnan et al. 2011; Yeh and Tallapragada 2012; Tallapragada et al. 2014; Mehra et al. 2018), the representation of TC track and intensity forecasts in dynamic models remains a challenge (Klotz and Nolan 2019). TC model forecasts and operational postprocessed best track from NOAA's National Hurricane Center (NHC) are generally available at standard synoptic times (0000, 0600, 1200, and 1800 UTC). However, they are not necessarily consistent with one another. Model output and the NHC best track use different definitions for TC intensity, i.e., the maximum wind speed at a height of 10-m above the surface (Vmax). The predicted TC intensity from an NWP model is normally defined as the instantaneous value of Vmax at a single model grid point (Tallapragada et al. 2014), which contains both small-scale spatial and temporal fluctuations. On the other hand, the NHC best track defines Vmax as the 1-min average based on available data. Vmax is further complicated by the fact that the time window varies by the TC operational forecast centers (OFCM 2012), with some centers using the 1-min average and others the 10-min average. Additionally, Vmax in the NHC best track shows appreciable discrepancies depending on the availability of satellite-, aircraft-, and land-based observations (Landsea and Franklin 2013). The inconsistency of data available to the NHC best track complicates the verification and evaluation of the forecast skill of TC models.

In the past decade, research and operational TC-based NWP models have become sophisticated with cloud-permitting resolutions, advanced physics parameterization schemes, improved inner-core data assimilation, and coupling to ocean and wave models. High-resolution TC models provide more opportunities for studying small-scale and TC inner-core features and for evaluating the high-frequency temporal evolution of TC track and intensity than low-resolution ones. While many researchers have investigated small-scale processes in high-resolution TC models (Gopalakrishnan et al. 2011, 2012, 2013; Bao et al. 2012; Tallapragada et al. 2014; Zhang et al. 2015, 2018), less attention has been devoted to the evolution of TC track and intensity as generated from high-resolution model output.

Traditionally, TC track and intensity forecast uncertainty in NWP models has been evaluated by introducing small perturbations to the initial conditions of an ensemble prediction system (Zhang 1997; Zhang and Krishnamurti 1997, 1999). Perturbations to large-scale flow and model physics have also been investigated (Lang et al. 2012; Zhang et al. 2014). Zhang et al. (2014) illustrated how perturbations in model initial conditions, the large-scale environment, and the choice of model physical parameterization schemes affect track and intensity forecasts from the Hurricane Weather Research and Forecasting (HWRF) Model. Grids in operational ensemble prediction systems generally have lower resolutions than those in their deterministic counterparts due to computer resource limitations and operational time constraints.

Corresponding author: Zhan Zhang, Zhan.Zhang@noaa.gov

DOI: 10.1175/MWR-D-21-0021.1

© 2021 American Meteorological Society. For information regarding reuse of this content and general copyright information, consult the AMS Copyright Policy (www.ametsoc.org/PUBSReuseLicenses).

Brought to you by NOAA Central Library | Unauthenticated | Downloaded 09/30/21 02:54 PM UTC

High-frequency temporal fluctuations have been explored in TC track and intensity forecasts from high-resolution models. Yang et al. (2020) showed that small-scale track oscillations, or trochoidal motions, were present in high-frequency track output from a high-resolution TC research model, comparable to observations (Jordan and Stowell 1955; Jordan 1966; Lawrence and Mayfield 1977). Klotz and Nolan (2019) recently showed that the fluctuation of intensity represented by Vmax from a TC model could be as large as ~15 m s^{-1} (29 kt) in a very short time period, which may induce large variations in the TC intensity forecast at synoptic times. Although dynamical models are now able to provide high-frequency and high-resolution TC track and intensity outputs, the current observing network is not extensive enough to provide accurate estimates of TC intensity variability due to undersampling in time and space. The TC intensity error caused by spatial undersampling in the current TC observing system has been studied and discussed in recent literature (Nolan et al. 2009; Uhlhorn and Nolan 2012; Nolan et al. 2013, 2014), but the issue of undersampling in time and its impact on the TC track and intensity forecast verification have not been addressed.

This study analyzes and evaluates the statistical characteristics of high-frequency TC track (location) and Vmax (intensity) from operational HWRF forecasts of North Atlantic TCs during 2017–19. The goal is twofold: 1) demonstrate and address the issue of temporal undersampling in TC model output and find an optimal representation of high-frequency TC track and intensity forecasts in comparison with model output of instantaneous track and intensity values at synoptic hours, and 2) identify, quantify, and investigate high-frequency variations in the operational HWRF track and intensity forecasts. The paper is organized as follows. The TC model used in this study along with the datasets are described in the next section. In section 3, the statistical characteristics and fluctuations associated with the high-frequency output of track, intensity, and radius of maximum wind (RMW) are analyzed, followed by summary and conclusions in section 4.

2. TC model and observation datasets

a. HWRF Model setup and high-frequency output

NOAA's operational HWRF modeling system is used in this study. The HWRF system is a cloud-permitting, high-resolution dynamical model that provides real-time track and intensity forecast guidance for active TCs over all global oceanic basins. It is widely used by operational TC forecast centers in the world, especially at NHC, the Central Pacific Hurricane Center (CPHC), and the Joint Typhoon Warning Center (JTWC). HWRF became operational at the Environmental Modeling Center (EMC) of the National Centers for Environmental Prediction (NCEP) in 2007 and, since then, has undergone significant upgrades (Tallapragada et al. 2014; Mehra et al. 2018). HWRF was developed based on the Nonhydrostatic Mesoscale Model (NMM) dynamic core of the WRF model with components specifically designed and tuned for TC prediction, including coupling to the ocean and wave models using a sophisticated NCEP coupler, vortex initialization and TC inner-core data assimilation for accurate representation of initial TC position, intensity, and structure, and a vortex tracker for deriving forecast parameters pertaining to TC track, intensity, and structure. In the North Atlantic and eastern North Pacific basins, HWRF uses the Message Passing Interface Princeton Ocean Model (MPI-POM, Yablonsky et al. 2015). Vortex initialization and data assimilation provides dynamic and thermodynamic balanced initial conditions (Tong et al. 2018).

The atmospheric model component of the HWRF system consists of three domains with horizontal resolution of 13.5 km for the outermost (parent) domain, 4.5 km for the intermediate domain, and 1.5 km for the innermost domain, and 75 levels in the vertical with hybrid sigma-pressure coordinates. The centers of the intermediate and innermost domains move to remain centered on the TC of interest. A scale-aware convective parameterization scheme (Han et al. 2017) is used for all model domains to resolve cumulus convection depending on domain resolution and can provide more spatially detailed and realistic TC structure. Evolution of a TC in the model is a result of interactions among the large-scale flows, mesoscale, and subgrid scale processes in the inner core region. HWRF physics parameterization schemes are carefully chosen and tuned in each model upgrade by performing multiseason retrospective experiments for the TCs occurring in the North Atlantic and eastern North Pacific basins.

HWRF is an on-demand TC forecast system that is able to start forecasts at the discretion of NHC, CPHC, and JTWC. HWRF provides 6-hourly TC forecast guidance out to 126 h for each cycle, with forecast data reported at synoptic times (0000, 0600, 1200, and 1800 UTC). The guidance includes model-predicted TC positions, instantaneous values of Vmax, minimum central sea level pressure (Pmin), and the 34-, 50-, and 64-kt (1 kt = 0.514 m s^{-1}) wind radii in each of the TC's four quadrants. This TC track and intensity guidance is provided in Automated Tropical Cyclone Forecasting (ATCF) format (Miller et al. 1990). A sophisticated vortex tracker algorithm developed by the Geophysical Fluid Dynamic Laboratory (GFDL) is used to extract the aforementioned information from the model post-processed output. The algorithm is briefly described here, and more details can be found in Marchok (2002). Twelve potential parameters are used in the algorithm to locate the TC center, including relative vorticity at 10 m above the ground, 850, and 700 hPa; mean sea level pressure (MSLP); geopotential height at 850 and 700 hPa; wind speed at 10 m, 850 hPa, and 700 hPa; and geopotential thickness for the 500–850-, 200–500-, and 200–850-hPa layers. Most of these parameters are drawn from the lower levels of the troposphere. The two upper-level geopotential thickness variables at the 200–500- and 200–850-hPa layers are used to maintain vertical coherence between the predicted TC center and model upper-level warm-core, which generally showed negligible impact on tracking results (Marchok, personal communication). The maximum or minimum value of each variable is first identified by applying a Barnes analysis (Barnes 1964) around the first guess TC center from the TCVitals, which is used by NCEP and many other modeling groups to begin the process of running a TC model and provided by NHC, CPHC, or JTWC for each TC at each synoptic hour. The predicted TC position will then be defined as an averaged location of all these maximum/minimum centers. The vortex tracker also reports on forecast data related to

Brought to you by NOAA Central Library | Unauthenticated | Downloaded 09/30/21 02:54 PM UTC

TABLE 1. Summary of TCs in 2017–19 Atlantic seasons (Total 45 TCs).

	<TS	TS	Category 1	Category 2	Category 3	Category 4	>Category 5	RI
2017	1	8	2	2	2	2	2	8
2018	1	7	3	3	0	1	1	6
2019	2	11	3	1	1	0	2	3
Total	4	26	8	6	3	3	5	17

TC intensity and wind structure. For MSLP, the value reported during the process of searching for the TC center was a smoothed value derived from the Barnes analysis. The tracker then analyzes the two-dimensional wind field to report on the TC intensity by searching for the maximum wind at 10 m within a 200-km radius of the identified TC center. This TC tracker algorithm will be referred to hereinafter as the GFDL tracker to distinguish it from the high-frequency tracking method described below.

In addition to TC track and intensity forecasts at synoptic hours, HWRF also provides high-frequency tropical cyclone forecast (HTCF) output at every model time step of the innermost domain, 10/3 s ($3\frac{1}{3}$ s). The output parameters include magnitude and location (i.e., latitude and longitude) of Vmax and Pmin. The locations of Pmin are generally collocated or close to the TC centers, especially for strong TCs, and therefore, can be utilized as high-frequency TC positions. The TC centers derived by the high-frequency locations of Pmin only will henceforth be referred to as the HTCF tracker. To compare the TC centers derived from the GFDL tracker and the HTCF tracker at the synoptic times, centered running means will be applied to the high-frequency Pmin-based tracker output. Note that there could be some differences in the estimated TC centers by the HTCF tracker and the GFDL tracker, especially for relatively weaker TCs (discussed in the next section). Running means with various time windows will be computed from high-frequency output to study the characteristics of small-scale TC track and intensity fluctuations.

The dataset used in this study includes all track and intensity forecasts from the 6-hourly GFDL tracker output and the high-frequency HTCF tracker output for 2017–19 North Atlantic TCs with the following classifications at the initial time and during forecast hours: subtropical depression (SD), subtropical storm (SS), extratropical cyclone (EX), tropical depression (TD), tropical storm (TS), and hurricane (HU). A total of 1131 independent forecasts are included in the dataset, of which 914 were initialized as TD/TS/HU. The Vmax values range from ~20 to 160 kt. In this study, only forecast cycles reported in the best tracks as TD, TS, and HU at the initial time are included in the TC intensity analysis and verification, and only forecast cycles for TCs initially with at least hurricane strength (≥64 kt) are included in the TC track analysis. Table 1 summarizes the number of TCs in different intensity categories based on the highest Vmax observed in a TC's entire life cycle in the best track.

b. Verification data

Two sets of observational data are used in this study. One is the observed 2-min TC center positions for Hurricanes Florence (2018) and Michael (2018). This dataset was created by the Hurricane Research Division (HRD) using the center fixes from multiple NOAA-P3 and Air Force C-130 missions, following the cubic-spline method of Willoughby and Chelmow (1982). The dataset is available from HRD (https://www.aoml.noaa.gov/hrd/data_sub/hurr.html). This dataset is used to compare high-frequency modeled track output for case studies of Hurricanes Florence (2018) and Michael (2018). Another observation dataset is from NHC's operational postseason best tracks (BEST), which are used for verification of the model TC track and intensity forecast errors. BEST is created from the real-time best tracks (b-decks) and after-season analysis done by TC forecasters and experts using more accurate information available after the TC season has completed each year. Normally, NHC updates BEST by March or April of the following year.

3. Analysis of high-frequency tropical cyclone forecast output

a. Track fluctuations

The HTCF tracker provides high-frequency TC positions based on minimum central pressure at every model time step. In contrast, the more sophisticated GFDL multivariable tracker is used to produce the official 6-hourly HWRF track forecast based on the instantaneous model state at specific synoptic times. Therefore, the TC track forecasts provided by the two methods could be different, especially for weak TCs. The HTCF tracker can capture track variations that occur on much shorter time scales than the GFDL tracker.

Figure 1 shows the predicted TC center differences produced by the HTCF tracker and the GFDL tracker, stratified by the strengths of the TCs using various thresholds based on the model predicted Vmax at the forecast lead times: weaker (35–44 kt) and stronger (45–63 kt) tropical storms (TS), category-1 (64–82 kt), category-2 (83–95 kt), and category-3 and stronger (>95 kt) hurricanes. It is evident from Fig. 1 that the predicted TC position differences identified by the HTCF tracker and the GFDL tracker are small, with a mean difference of less than 8 km for the above hurricane-strength (≥64 kt) TCs, and 10 km for stronger TS (45–63 kt). Overall, the position differences become larger for weaker TCs. For example, the position differences are ~20 km for TCs whose Vmax values are between 35 and 44 kt. The reason that the TC position difference becomes larger for weaker TCs is mainly that the TC positions from the HTCF tracker are contaminated by the possibility of multiple Pmin centers, while the multivariate algorithm of the GFDL tracker produces more accurate positions for weaker TCs. To ensure similar TC positions from the HTCF and GFDL

Brought to you by NOAA Central Library | Unauthenticated | Downloaded 09/30/21 02:54 PM UTC

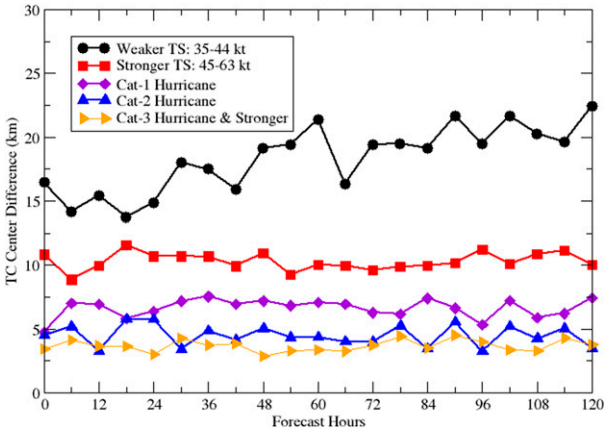

FIG. 1. The TC position differences between the HTCF tracker and the GFDL tracker are compared at various TC intensities: weaker tropical storms (black), stronger tropical storms (red), category-1 hurricanes (purple), category-2 hurricanes (blue), and category-3–5 hurricanes (orange).

trackers, the TC track analysis and verification performed in this study focused mainly on TCs initially with at least hurricane strength (≥64 kt).

Hurricane Florence (2018) and Hurricane Michael (2018) results are used to illustrate typical characteristics of high-frequency TC tracks from HWRF output. Both TCs made landfall in the United States, and HRD flight-level airborne observations were available when these TCs approached the U.S. coastline. Track forecasts, using the HTCF tracker and the 6-hourly GFDL tracker, are compared for Hurricane Florence (Figs. 2a,b) and Hurricane Michael (Figs. 2c,d). Hurricane Florence forecasts were initialized at 0000 UTC 9 September 2018 and Hurricane Michael forecasts were initialized at 1200 UTC 8 October 2018. These track forecasts are also compared with two sets of observed tracks in Fig. 2: BEST and HRD's 2-min tracks (see section 2b). A 30-min running mean was applied to the HTCF tracker output to smooth the track forecasts.

Trochoidal motion, described by circular motion around a moving center, has been previously observed for TC tracks in radar (Jordan and Stowell 1955; Jordan 1966), satellite (Lawrence and Mayfield 1977), and flight-level data (Marks et al. 2008; Aberson et al. 2017). Nolan and Montgomery (2000) found that TC trochoidal motion can be described as an algebraic azimuthal wavenumber-one instability in the framework of two-dimensional, nondivergent, inviscid vortices on an f-plane. Using that idealized framework, they derived a closed form solution describing the evolution of linearized wavenumber-one disturbances. Nolan et al. (2001) demonstrated that trochoidal motions can also be induced by the exponential wavenumber-one instability in a framework of two-dimensional, divergent flows on an f-plane. Based on their derivation, the wavenumber-one instability was found to occur in annular vortices that resemble TCs. The rotational period of the trochoidal motion was found to be slightly less than $2\pi/\Omega\text{max}$, where Ωmax is maximum angular velocity.

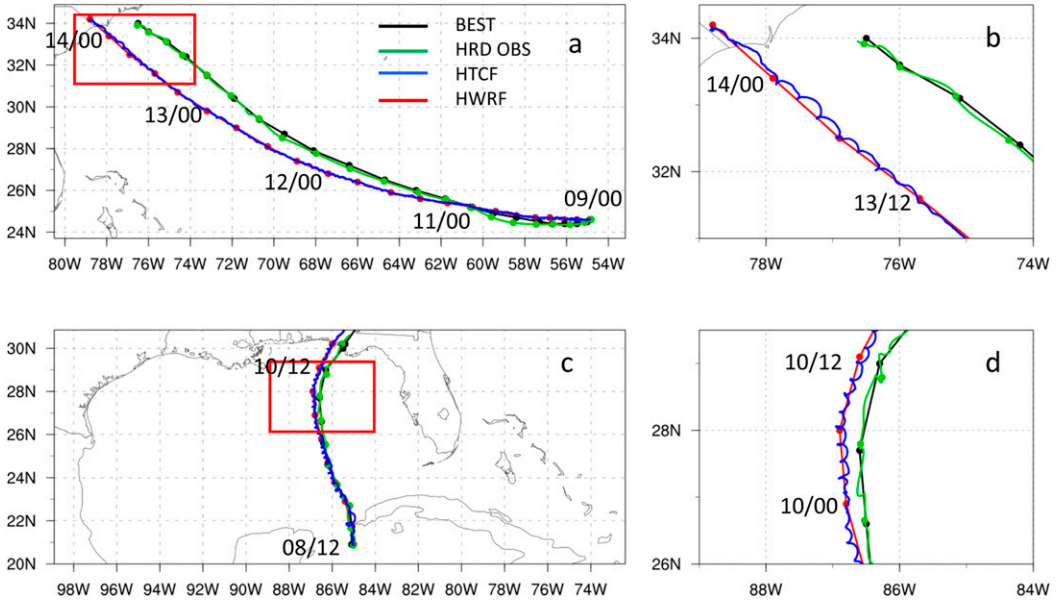

FIG. 2. HWRF track forecasts for (a),(b) Hurricane Florence initialized at 0000 UTC 9 Sep 2018 and (c),(d) Hurricane Michael initialized at 1200 UTC 8 Oct 2018. (left) Two observed tracks, the NHC best track (black) and HRD storm track constructed by cubic-spline smoothing (green), and two forecast tracks, operational HWRF (red) and HWRF high-frequency (blue), are compared. (right) Track forecasts zoomed in to the area of interest outlined in red in (a) and (c). Note that the HRD storm track was created following Willoughby and Chelmow (1982) and is plotted here for reference. Circles show TC positions every 6 h for the NHC best track (black) and the operational HWRF (red).

Brought to you by NOAA Central Library | Unauthenticated | Downloaded 09/30/21 02:54 PM UTC

TABLE 2. Comparison of rotational periods from HWRF using the HTCF tracker and theoretical values based on previous studies (Nolan and Montgomery 2000; Nolan et al. 2001).

	Vmax (m s^{-1})	Rmax (km)	Ωmax ($\times 10^{-3}$ s^{-1})	$2\pi/\Omega$max (min)	Model rotational period (min)
Florence	59	50	~1.18	89	~100
Michael	49	33	~1.48	71	~80

Trochoidal-like motion was seen in high-frequency track forecasts from HWRF and HRD flight-level data for Hurricanes Florence (2018) and Michael (2018, Fig. 2). In HWRF forecasts, small-scale, counterclockwise motions were apparent in the HTCF tracker that oscillated around the low-frequency track as captured by the GFDL tracker (Figs. 2a,c). The rotational periods of these oscillations simulated by HWRF, derived from the HTCF tracker, was ~80 min (~9 cycles in 12 h) for Hurricane Michael and ~100 min (~7 cycles in 12 h) for Hurricane Florence. For both TCs, the rotational periods from the HCTF tracker are in reasonable agreement with the theoretical rotational periods for trochoidal motion based on wavenumber-one theory (Table 2). The values of Vmax and Rmax in Table 2 are 12-h HTCF mean values between 84–96 h for Hurricane Florence and 36–48 h for Hurricane Michael. However, HWRF is a complex nonhydrostatic TC forecast system with presence of moisture, baroclinicity, and other subgrid parameterizations. These nonlinear processes, in particular, moisture and strong convergent flows, make it difficult to determine if the high-frequency track oscillations from HWRF are, in fact, the theoretical trochoidal motions described in Nolan et al. (2001) given the available output. The annular shape vortex with wavenumber-one structure at the vortex core was confirmed at multiple vertical levels (up to 300 hPa; not shown). The growth-rates of various azimuthal wavenumber asymmetries of the vorticity fields were examined, showing that the wavenumber-one component dominates over the rest of the asymmetries and all grow with time, which infers consistency with the theory. However, whether there is an instability that grows linearly with time is unknown at this stage due to limited parameters in the operational model output. The current analysis is only intended to show that HWRF is capable of producing small-scale TC track oscillations that are similar to theorized trochoidal motions. Further study and analysis are required to investigate the details of TC trochoidal motions in the research version of HWRF forecasts, a topic that is outside the scope of this study.

In HRD flight-level data, TC center positions were constructed by cubic-spline smoothing (Willoughby and Chelmow 1982), revealing wobbles that resemble trochoidal motions (Marks et al. 2008; Aberson et al. 2017). The number of TC center fixes conducted by the aircraft affects the estimated scales or frequency of the trochoidal-like motion that can be resolved. When the aircraft circles within the eye of Hurricane Hugo (1989) for a relatively long period (see Fig. 6a of Marks et al. 2008), several trochoidal loops in the storm track were observed, and the estimated periods of these loops were in agreement with the theory. Only from four to six eyewall penetrations were conducted over the course of several hours in Florence and Michael, leading to smoother storm tracks relative to the Hugo track. As a result, the rotational periods of trochoidal-like motions in the HRD observed tracks of Florence and Michael (Figs. 2b and d) are larger than that calculated based on the HWRF high-frequency output following the theory on trochoidal motions.

Next, all track forecast outputs from the HTCF tracker were examined for TCs over a three-year period (2017–19), including the magnitudes of track fluctuations, the dependence of those fluctuations on Vmax, and impact on the accuracy of the track forecasts. Track fluctuations are defined as the distances between the high-frequency TC positions from the HTCF tracker and the corresponding 1-h (±30 min) running mean of the HTCF tracker output. The distribution of track fluctuations for hurricanes (Vmax ≥ 64 kt) was analyzed for four groups based on the model-predicted TC intensities: 1) category 1 (64–82 kt), 2) category 2 (83–95 kt), 3) category 3 (96–112 kt), and 4) category 4 and stronger (≥ 113 kt). Track fluctuations and TC intensity are inversely proportional, with stronger TCs associated with smaller mean track fluctuations, and vice versa (Fig. 3). For category-4 and stronger hurricanes, track fluctuations had a mean and standard deviation of ~6 and ~3 km, respectively, whereas, for category-1 hurricanes, these values were ~8 and ~7 km, respectively. This implies that track fluctuations have less impact on the track forecast errors of stronger TCs than they do on weaker TCs. In other words, when a TC becomes stronger, its track is likely to be more stable with smaller fluctuations. To show the details of track fluctuations for an individual TC, the forecast of Hurricane Florence initialized at 0000 UTC 9 September 2018 was examined (Fig. 4). Average track fluctuations were ~8 km and the maximum fluctuation was greater than 20 km (Fig. 4a). Track fluctuations exhibited notable variability throughout the forecast period, with smaller fluctuations at 12–60-, 78–90-, and 96–102-h lead times and larger fluctuations at 60–78-, 90–96-, and 102–120-h lead times. Track fluctuations for Florence were further investigated in a 24-h period (24–48 h lead times) in the same forecast (Fig. 4b). Track fluctuations were smoothed by applying a 1-h running mean, revealing ~60–80-min oscillation period for this particular time period. Note that Vmax and Rmax were different for this period than what was shown in Table 2, so the oscillation period may not be the same.

The distribution of TC track fluctuations was related to TC intensity, although the most common track fluctuation was 4–8 km for all hurricanes (Fig. 5). Furthermore, at least 80% of hurricanes are associated with track oscillations of less than 12 km (i.e., the summation of the first three bars in Fig. 5). In general, weaker hurricanes have higher track oscillations than stronger hurricanes, with fluctuations in category-1 and category-2 hurricanes as high as 40 km (Figs. 5a,b). The impact of small-scale

Brought to you by NOAA Central Library | Unauthenticated | Downloaded 09/30/21 02:54 PM UTC

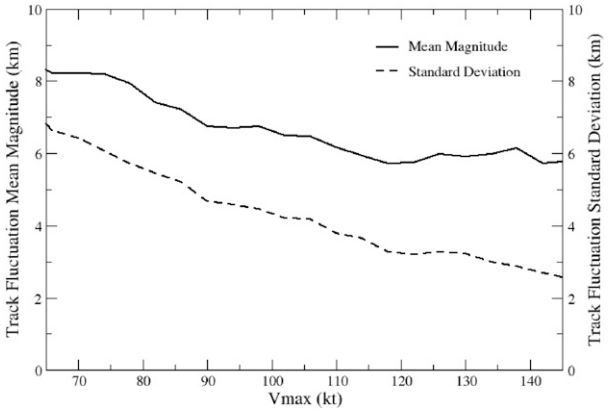

FIG. 3. The mean (solid line; left *y* axis) and standard deviation (dashed line; right *y* axis) of track fluctuations (km) as a function of maximum intensity (Vmax; kt) for all North Atlantic hurricanes (Vmax ≥ 64 kt) from the 2017–19 hurricane seasons.

track fluctuations on track forecast verification will be discussed in section 3d.

b. *Intensity fluctuations*

To avoid the impact of land on the intensity forecast analysis, the running-mean method was only applied to Vmax from the HTCF tracker when a TC was at least 3 h away from the coastline. The conventional 6-hourly intensity values at synoptic times from HWRF were used when a TC was close to land and after landfall. Temporal Vmax fluctuations were explored in 5-day forecasts of Hurricane Florence initialized at 0000 UTC 9 September 2018 (Figs. 6a,b) and Hurricane Michael initialized at 0000 UTC 8 October 2018 (Figs. 6c,d). TC Vmax forecasts were compared for the GFDL tracker (every 3 h), the HTCF tracker at every model time step ($3^1/_3$ s), a 60-min running average of the HTCF tracker, and a 360-min running average of the HTCF tracker. It is worth noting that although a relatively large fluctuation (~20 kt) exists in Vmax (Figs. 6b,d), fluctuations in Pmin are relatively small (~4 hPa; not shown). When smoothing over smaller time windows (≤60 min), these time series appear to be very similar to the raw high-frequency HTCF output. Conversely, the 360-min (i.e., ±3-h window) running-mean time series was much smoother and was generally similar to the 6-h GFDL tracker output provided to NHC as official forecast guidance. The timing of rapid intensification (RI) might be impacted in these running-mean time series, as indicated by forecast hour 21 when Hurricane Florence was completing its RI period in the GFDL tracker and just starting its RI period in the 360-min running-mean time series (Fig. 6b). The raw HTCF tracker output showed a much sharper increase to Vmax that occurred between forecast lead times of 20–21 h. RI in the GFDL tracker may have been artificially slow due to coarse temporal resolution. Note that the Vmax fluctuations shown here are consistent with those found in WRF simulations in Klotz and Nolan (2019). It is interesting how the low-frequency and high-frequency time series tell different stories about the evolution of Vmax. The 3-hourly GFDL tracker output provides a steady snapshot of instantaneous TC intensity

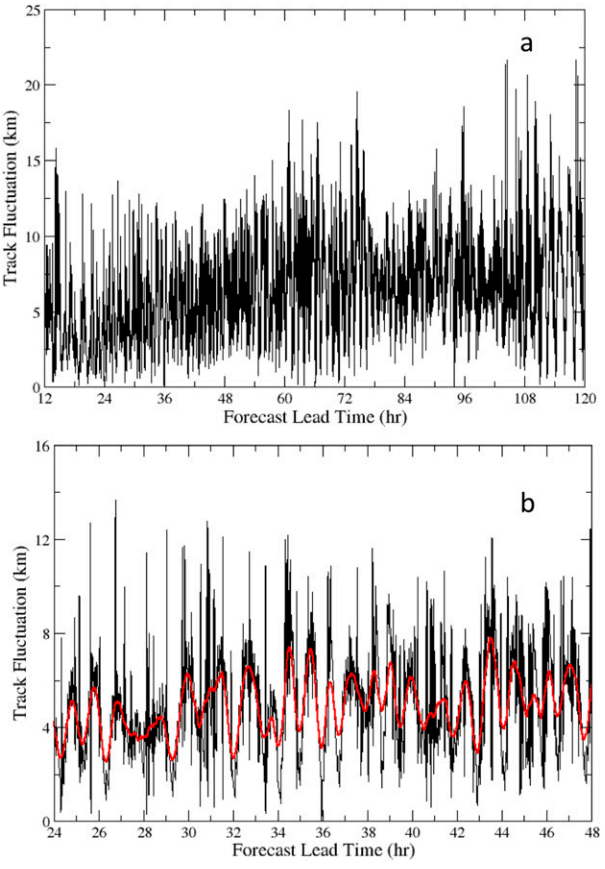

FIG. 4. (a) High-frequency ($3^1/_3$ s) track fluctuations (km) for 12–120-h forecast lead times from an HWRF forecast for Hurricane Florence initialized at 0000 UTC 9 Sep 2018. (b) As in (a), but for 24–48-h forecast lead times. The corresponding 1-h running mean (red) is overlaid in (b).

from HWRF. However, the HTCF tracker output suggested that the model-predicted Vmax constantly fluctuated, so the 3-hourly Vmax value could occur in a peak or valley of those fluctuations. For example, the RI period of Hurricane Florence was more complex in the HTCF tracker than in the GFDL tracker, with an initial Vmax increase from 18.5 to 19.5 h, a slight decrease in Vmax from 19.5 to 20 h, and a more rapid Vmax increase from 20 to 21 h. The HTCF tracker output indicates that Vmax fluctuations exist on subhourly time scales that may be important to contextualize TC forecast guidance from high-resolution models.

To study the general characteristics of the intensity fluctuations, a similar approach to the TC track fluctuation analysis was used. The differences between the high-frequency (every $3^1/_3$ s) Vmax and the corresponding 6-h (±3-h window) running means are first computed for all TCs from 2017 to 2019. The results are categorized into several groups based on TC intensity and classification, and the absolute values of the Vmax intensity differences are then averaged for each group. Figure 7 shows the standard deviation of Vmax variations as a function of TC intensity based on a composite analysis for various TC intensities and classifications. For tropical storms and minimal hurricanes (<85 kt), Vmax fluctuations increase as Vmax

Brought to you by NOAA Central Library | Unauthenticated | Downloaded 09/30/21 02:54 PM UTC

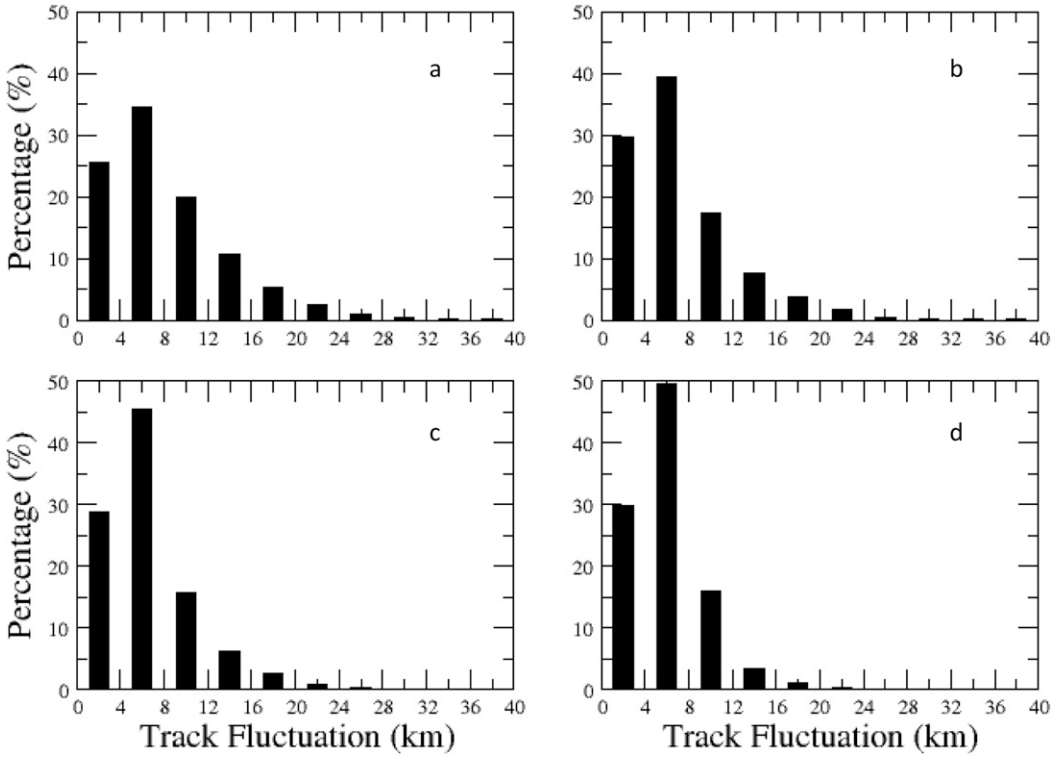

FIG. 5. Histograms show TC track fluctuations (km) binned every 4 km for (a) category-1 hurricanes, (b) category-2 hurricanes, (c) category-3 hurricanes, and (d) category-4 and category-5 hurricanes.

increases, starting from ~2.5 kt for minimal tropical storms and reaching a peak fluctuation of 5.5 kt when the Vmax is 90 kt (i.e., category-2 hurricane). For higher values of Vmax, intensity fluctuations gradually decrease in magnitude to near 2.5 kt for very strong TCs (Fig. 7). Interestingly, minimal tropical storms exhibit a similar variance of Vmax fluctuations as TCs stronger than category 4. The small Vmax variations for weaker TCs can be explained by the relatively small values of corresponding Vmax; that is, Vmax fluctuations are limited by weak Vmax. On the other hand, Vmax variations gradually decrease for major hurricanes.

The distribution of Vmax fluctuations is explored in various model-predicted TC intensity classifications (Fig. 8). The percentage of near-zero Vmax fluctuations (i.e., when high-frequency Vmax approximately matches low-frequency Vmax at specific synoptic times) is between 22% and 30% for all tropical storms and hurricanes, with the highest percentage (29.2%) for category-4/5 hurricanes. Category-2 hurricanes had the largest Vmax fluctuations and had the lowest percentage of near-zero Vmax fluctuations (22.1%), further confirming that the high-frequency Vmax fluctuates the most for category-2 hurricanes. Based on the analysis above, the intensity forecasts taken at one single model grid point from the operational HWRF at a specific instant may not be a good representation of the Vmax in comparison with BEST because that instantaneous Vmax value could occur when Vmax fluctuations are nonzero. The running mean of the high-frequency intensity output at 6-h time windows (±3 h) is as smooth as the official HWRF Vmax forecasts at 6-hourly synoptic times (cf. Fig. 6). Intensity forecasts will be verified in section 3d.

c. Vmax *location and intensity changes*

The HTCF data also include the predicted position of Vmax, from which the distance between the TC center and the location of Vmax can be calculated. Note that the high-frequency distance to maximum winds (DMW) is similar, but not identical, to RMW that is defined as the radius where the azimuthally averaged wind speed is greatest. The high-frequency TC centers and DMW from Hurricane Florence forecast initialized at 0000 UTC 9 September 2018 are shown in Fig. 9a. The Vmax was generally located to the right side of the TC motion vector, which makes sense given that the TC circulation and the large-scale steering flow add constructively to one another on that side of the cyclone. High-frequency Vmax positions exhibited trochoidal motion similar to that observed in high-frequency TC center positions (cf. Fig. 2), except the Vmax location oscillations had larger spatial and temporal scales than the TC center oscillations.

TC RI, defined as when Vmax increases by at least 30 kt in 24 h (Kaplan and DeMaria, 2003; Kaplan et al. 2010), is one of the most challenging problems in TC prediction (Fischer et al. 2019). Figure 9b shows the time evolution of the predicted high-frequency Vmax together with DMW for the Florence forecast. Hurricane Florence was predicted to go through a RI during the forecast period (lead times of 12–36 h), gradual intensification (36–72 h), and near-steady and gradual weakening

Brought to you by NOAA Central Library | Unauthenticated | Downloaded 09/30/21 02:54 PM UTC

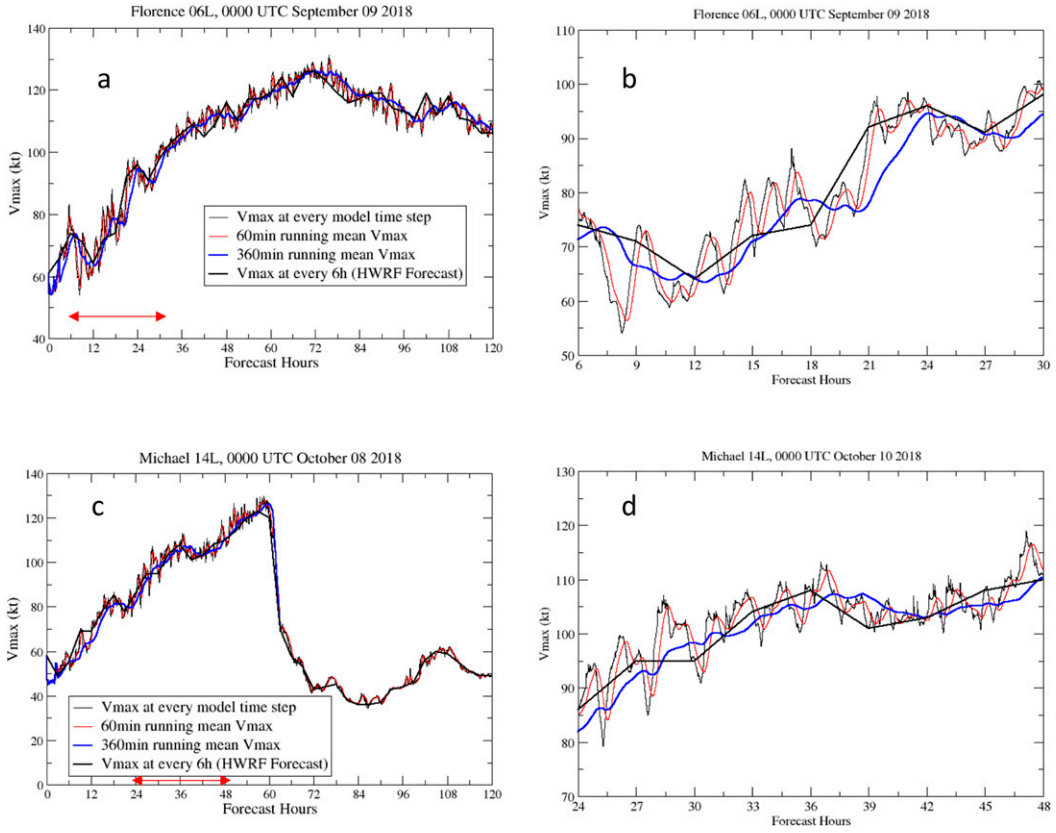

FIG. 6. The Vmax from HWRF forecasts of (a),(b) Hurricane Florence initialized at 0000 UTC 9 Sep 2018 and (c),(d) Hurricane Michael initialized at 0000 UTC 8 Oct 2018 for (left) the entire 5-day forecast period and (right) the specific 24-h periods indicated by red arrows in (a) and (c).

(72–120 h). This intensity evolution allowed us to investigate the possible relationship between Vmax and DMW variations and TC intensity change. DMW shrunk before the onset of RI (lead times up to 12 h) with large fluctuations and remained steady state during the RI period. Interestingly, DMW continued to grow even as Florence intensified. DMW fluctuations clearly increased in amplitude as Florence began to weaken (lead times longer than 72 h). For this case, DMW fluctuations were as large as 25 km (~16 model grid points) in one hour. The linear fit of Vmax fluctuations for a Hurricane Florence forecast initialized at 0000 UTC 9 September 2018 showed three distinct periods: prior to RI, RI, and steady state (Fig. 10). It is evident that Vmax fluctuations were larger before RI, linearly decreased during the RI period, and finally remained smaller in the subsequent intensification period.

The relationship between Pmin center (i.e., TC center) fluctuations and corresponding Vmax center fluctuations was investigated for different TC categories using a composite analysis method (Fig. 11). The composite data were generated by averaging HTCF Pmin center fluctuations and Vmax center fluctuations for hurricanes at each 30-min interval throughout the entire 5-day forecast. The data were then stratified into four groups based on Vmax: 1) category-1 hurricanes, 2) category-2 hurricanes, 3) category-3 hurricanes, and 4) category-4 and stronger hurricanes. In general, stronger TCs had less TC position fluctuations than weaker TCs. The correlation coefficients between the TC center fluctuations and Vmax center fluctuations were ~22% and 34% for category-3 and category-4 storms, respectively, indicating that larger TC Pmin center position variations were associated with larger Vmax center position variations for these TC categories. There is no clear relationship between Pmin center fluctuations and Vmax center fluctuations for TCs weaker than category 2.

It is well established that TC RI is generally accompanied by a reduction in RMW, also known as storm contraction (Willoughby 1990; Liu et al. 1999; Yau et al. 2004; Rogers 2010, Qin et al. 2016; Zhang and Rogers 2019). Figure 12 compares 24-h changes of Vmax and RMW from using BEST and 24-h changes of Vmax and DMW from HTCF data. It is worth mentioning that the RMW data in BEST are not postanalyzed by NHC because they are largely based on operational estimates. BEST shows that the 24-h RMW changes are either near zero or negative for RI events and are either near zero or positive for rapid weakening events (Fig. 12). In other words, a TC either maintains or shrinks its size when it undergoes RI, whereas it either maintains or grows its size during periods of rapid weakening. This result is consistent with Stern et al. (2015). The relationship between the 24-h tendencies of Vmax and RMW for RI and rapid weakening events in DMW from the HTCF tracker was similar to that in BEST (Fig. 12). That

Brought to you by NOAA Central Library | Unauthenticated | Downloaded 09/30/21 02:54 PM UTC

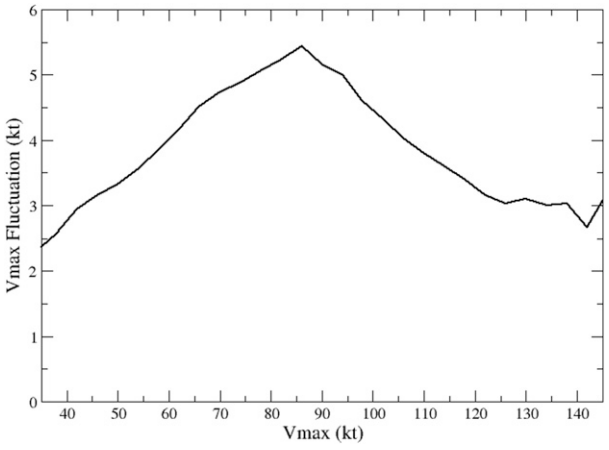

FIG. 7. The standard deviation of maximum intensity (Vmax) fluctuations (kt) as a function of Vmax (kt). All TCs from the 2017–19 North Atlantic hurricane seasons that were classified as TS or stronger (Vmax ≥ 34 kt) were included in the sample.

said, DMW from the HTCF tracker exhibited much larger tendencies (>250 km per 24 h) relative to the RMW values in BEST (<200 km per 24 h). Of course, the definitions for RMW and DMW are different, so that could partly explain differences in the fluctuations. Other possibilities to explain differences in storm size fluctuations are: 1) the operational HWRF generally overpredicts the TC size, leading to larger TC size fluctuations in the HTCF data for intensifying and weakening TCs; 2) DMW (and likely RMW) have more fluctuations than previously thought that are not captured in BEST at the synoptic times; and 3) the vast majority of TCs lack sufficient observational data to accurately calculate RMW, especially those that are not sampled by aircraft reconnaissance.

d. Verification for running-mean track and intensity forecasts using HTCF data

As mentioned in section 2a, BEST was used as truth for TC track and intensity in this study. BEST generally reflects only an estimate of temporally averaged TC positions and intensity, especially when aircraft data are unavailable (Landsea and Franklin 2013). In BEST, a latitude and longitude location for a TC is provided only at specific synoptic times (i.e., 0000/0600/1200/1800 UTC), and it does not typically capture small-scale oscillations due to its coarse temporal resolution (6 h). It is important to note that BEST positions are somewhat subjectively smoothed, and, as a result, they may not exactly match the locations observed by high-resolution aircraft center fixes at a given synoptic time. For more details, see section 2 of Landsea and Franklin (2013). Furthermore, Vmax values in BEST represent averaged maximum sustained winds over a certain time period near the synoptic time (e.g., 1200 UTC), rather than the instantaneous intensity at the exact synoptic time (Landsea and Franklin 2013). While NHC uses 1-min maximum sustained winds to describe the TC intensity, other international TC forecast centers such as the Japan Meteorological Agency and the Chinese Meteorological Administration use 10-min maximum sustained winds (Harper et al. 2010). Similarly, the instantaneous values produced every 6 h from the operational HWRF are not able to capture high-frequency temporal fluctuations that are important to understand how the model represents TC motion and intensity.

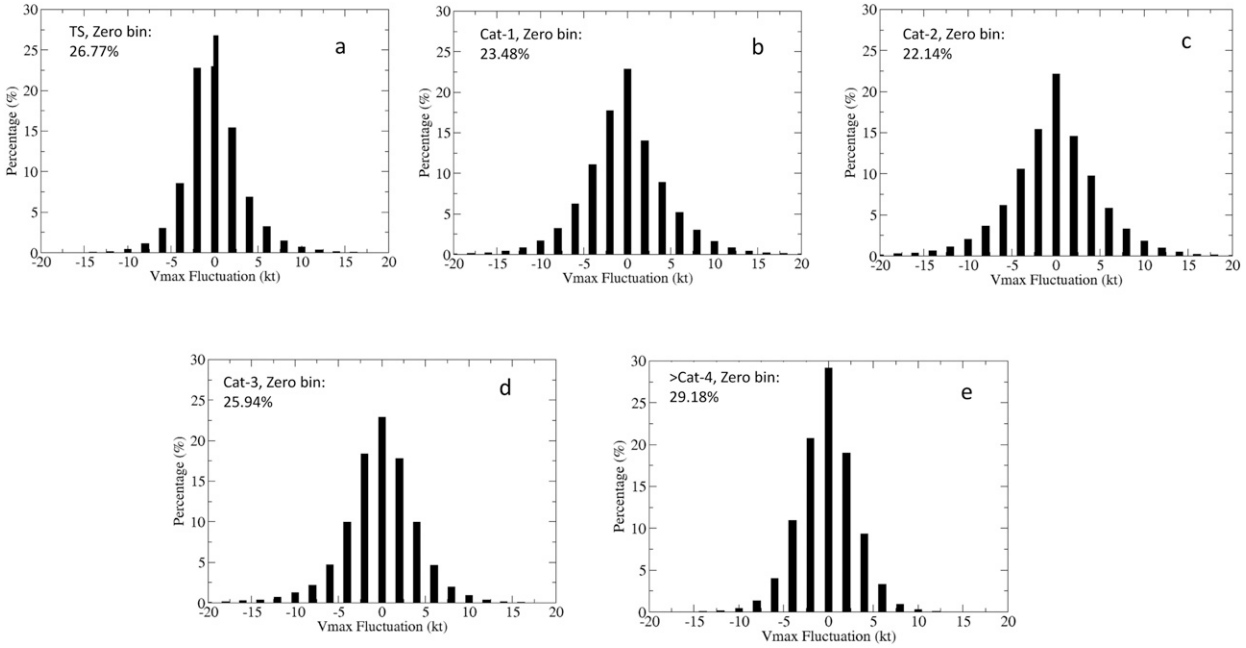

FIG. 8. Histograms of TC Vmax fluctuations from 6-h running mean for different TC classifications: (a) tropical storms, (b) category- 1 hurricanes, (c) category-2 hurricanes, (d) category-3 hurricanes, and (e) category-4 and category-5 hurricanes.

Brought to you by NOAA Central Library | Unauthenticated | Downloaded 09/30/21 02:54 PM UTC

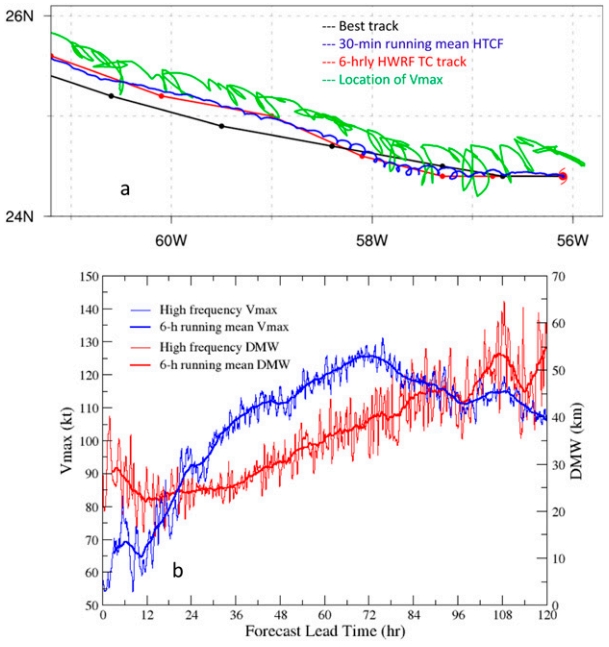

FIG. 9. Track, maximum 10-m wind speed (Vmax), and radius of maximum winds (RMW) for an HWRF forecast of Hurricane Florence initialized at 0000 UTC 9 Sep 2018. (a) Track forecasts are compared from the operational 6-hourly GFDL tracker (red), 30-min running mean of the HTCF tracker (blue), NHC best track (black), and the Vmax location from the HTCF tracker (green). The NHC best track and the operational 6-hourly GFDL tracker are marked every 6 h by a circle. (b) Forecasts of Vmax (blue) and the distance to maximum winds (DMW; red) are compared, with thin lines representing the 30-min running mean and thick lines representing the 6-h running mean.

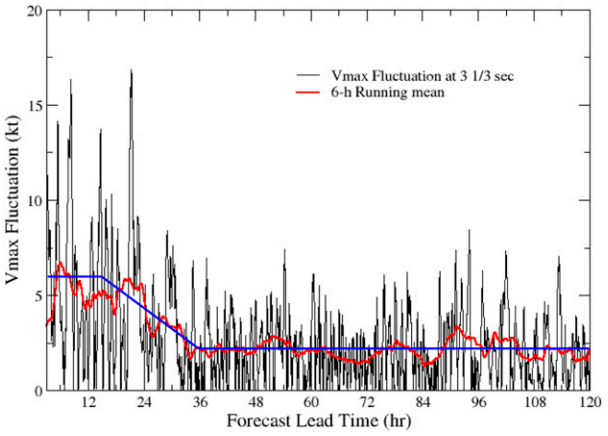

FIG. 10. Maximum intensity (Vmax) fluctuations for a 5-day HWRF forecast of Hurricane Florence initialized at 0000 UTC 9 Sep 2018. The black line represents high-frequency ($3^1/_3$ s) fluctuations, the red line represents the 6-h running mean of high-frequency fluctuations, and the blue line represents the linear best fit for the three distinct periods in the TC life cycle: prior to RI (0–12 h), RI (12–36 h), and steady-state/weakening (36–120 h).

In fact, the instantaneous values from HWRF sometimes could be outliers that become difficult to compare with the smoothed values from BEST. It is expected that the model-predicted track and intensity will be more consistent with those in BEST if these small-scale temporal fluctuations are removed from modeled high-frequency outputs.

To estimate the impact of temporal fluctuations in the high-frequency outputs on HWRF's forecast performance, TC track and intensity verifications were performed against BEST for all 2017–19 North Atlantic TCs. The following model products are compared with each other: the operational HWRF 6-hourly output from the GFDL tracker (HWRF) and the HTCF tracker output averaged over a 3-h (±1.5-h) time window (180M), a 6-h (±3-h) time window (360M), and a 9-h (±4.5-h) time window (540M). The track and intensity verification for the operational HWRF will be used as a baseline to compute forecast skill scores for 180M, 360M, and 540M. Therefore, the forecast track and intensity skill scores for each model product are calculated as follows:

$$\text{Skill Score} = \frac{E_{\text{HWRF}} - E_{\text{model}}}{E_{\text{HWRF}}},$$

where E_{HWRF} denotes the average forecast error from HWRF and E_{model} denotes the individual forecast errors from high-frequencyproducts, that is, 180M, 360M, and 540M. A positive skill score indicates improved performance for a given product relative to the standard HWRF output, and vice versa.

The track forecast skill was similar at most of the forecast lead times among the operational HWRF, 180M, 360M, and 540M, except for an ~3% improvement in the track forecast skill from 540M over the operational HWRF at early forecast lead times (not shown). Track forecasts were only verified for TCs of at least hurricane intensity at the model initialization time (≥64 kt) because TC center positions from the HTCF tracker and the GFDL tracker were small for those intensities. This result was expected because the spatial scale of fluctuations caused by trochoidal motions was too small to have a meaningful impact on the large-scale TC movement (see section 3a).

Verification of intensity forecasts from smoothed HTCF tracker output showed notable improvements over HWRF at all lead times (Fig. 13). Intensity forecasts were verified for all TCs that were reported as SD, SS, TD, TS, and HU in BEST at the model initialization time. For all TCs, intensity forecast skill scores for 360M and 540M showed at least ~2%–8% improvements over the operational HWRF Vmax forecasts at all lead times, with higher skill scores at shorter lead times (Fig. 13a). 180M intensity forecast skill scores were positive (up to 4%) at every forecast lead time as well. The verification was then stratified for weaker TCs ($34 \leq \text{Vmax} < 64$ kt) and stronger TCs (≥64 kt), with similar results (Figs. 13b,c). All three intensity products that used running means of the high-frequency intensity forecasts outperformed the operational HWRF for both weaker and stronger TCs, with higher intensity forecast skill improvements for weaker TCs than for stronger TCs. Interestingly, a larger running-mean time window (i.e., 540M) produced slightly more skillful results than smaller time windows (i.e., 360M and 180M) at all forecast lead

Brought to you by NOAA Central Library | Unauthenticated | Downloaded 09/30/21 02:54 PM UTC

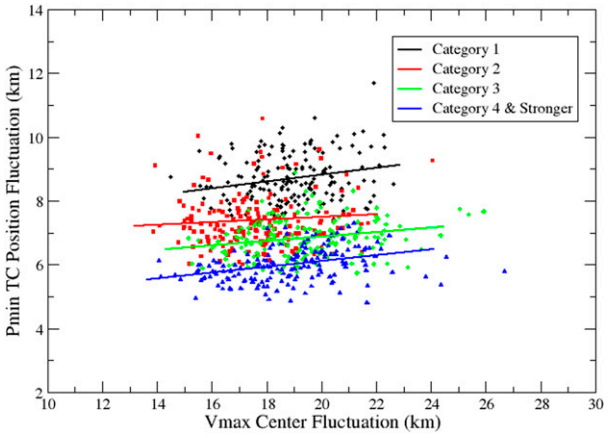

FIG. 11. A scatterplot for composited Pmin TC Center fluctuations vs TC Vmax center fluctuations around a 60-min running mean. The composite data were generated by averaging TC position fluctuations and Vmax center fluctuations for hurricanes at each 30-min interval throughout the entire 5-day forecast. Data for four TC classifications are shown: category-1 hurricanes (black asterisk), category-2 hurricanes (red square), category-3 hurricanes (green diamond), and category-4/5 hurricanes (blue triangle).

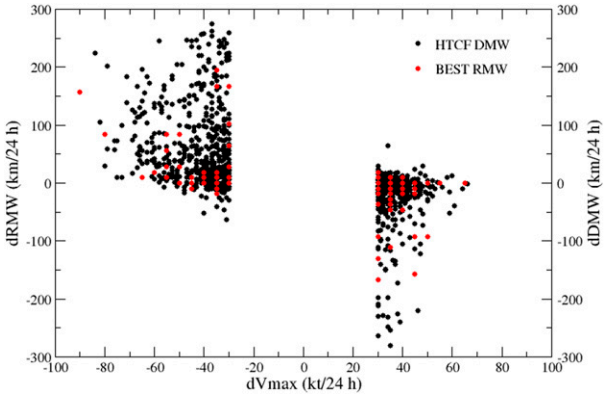

FIG. 12. A scatterplot of Vmax tendencies vs RMW tendencies from BEST (red) and Vmax tendencies vs DMW tendencies from the HTCF tracker (black). All tendencies have units of kilometers per 24 hours.

times. It is worth noting that the running mean is not applied 3 h prior to and after TCs make landfall, such that the running-mean approach should not affect the accuracy of TC intensity forecasts for landfalling TCs. Because the dynamic model guidance is usually delivered to the forecast center later than other model guidance, an ''early'' version of the dynamic model is interpolated from the previous model forecast to provide real-time forecast guidance to NHC and other operational centers. An early version of 360M intensity forecasts was computed and compared with the official early version of HWRF intensity forecasts. The verification shows that there was not much difference between the two interpolated versions (not shown). The early model version uses the TC intensity difference between the 6-h forecast from the previous cycle and current best track data to adjust and correct the predicted intensity at longer forecast lead times. Since, in general, the intensity difference between the GFDL tracker and the 6-h running mean of the HTCF tracker was small relative to the intensity offset applied at that time, the same bias correction was applied to compute the early version of HWRF and 360M. This could explain why the running-mean method does not affect the early model verification.

The impact of high-frequency running mean on the late model TC intensity forecasts was examined in Fig. 14 by only verifying the forecast cycles in which RI occurred (DeMaria and Franklin 2019). It shows that the intensity forecast skill scores for the RI forecasts improved at all forecast lead times up to 72 h, with the largest improvements occurring at 36 and 72 h, when running-mean intensity forecasts using HTCF data were up to 8% more skillful than the intensity forecasts produced by the operational HWRF. The exception was 540M at 24 h, which showed an insignificant degradation.

The 6-h TC intensity changes predicted by 180M, 360M, 540M, and HWRF were also verified against BEST (Fig. 15). The 6-h intensity change is an important verification metric because it helps diagnose if the model predicts TC intensification, weakening, or steady state at the right time. By applying a running mean to the high-frequency HWRF outputs to remove small-scale intensity fluctuations, the errors of 6-h intensity change were reduced by ~2 kt. The verification results indicate that the larger the average time window, the closer the predicted Vmax values were to BEST. However, since Vmax in BEST is reported every 6 h, it is not desirable to apply a time window greater than this time interval because that would impact the timely delivery of these datasets as forecast guidance. Thus, analysis focuses on the 360M intensity verification hereinafter.

The 6-h intensity change histogram at 24, 72, and 120 h from HWRF, 360M, and BEST were compared in Fig. 16. It can be clearly seen that for all forecast lead hours, the 360M 6-h intensity change histogram was closer to that of BEST than HWRF, especially in terms of the percentage of cases in the bins from −5 to 5 kt. In addition, the HWRF distribution was broader than 360M and BEST, with a higher-than-expected percentage of large intensity change values (i.e., >15 or <−15 kt). These results provided guidance on how the operational HWRF track and intensity forecasts could be improved with existing model output and provided valuable information on the variations associated with Vmax predictions. The intensity forecasts generated by an earlier version of 360M, which applied the 6-h running mean to HTCF without taking account for landfall impact, was implemented in 2020 operational HWRF and were provided to NHC as an additional HWRF intensity forecast guidance. A new version of 360M based on the results from this study is planned to be implemented during the next HWRF upgrade, which applies the 6-h running mean to HTCF until the TC moves within 3 h of landfall in the forecast.

4. Conclusions

In this study, the high-frequency ($3\frac{1}{3}$ s) outputs of TC track and intensity forecasts were analyzed from the operational HWRF system for the 2017–19 North Atlantic hurricane

Brought to you by NOAA Central Library | Unauthenticated | Downloaded 09/30/21 02:54 PM UTC

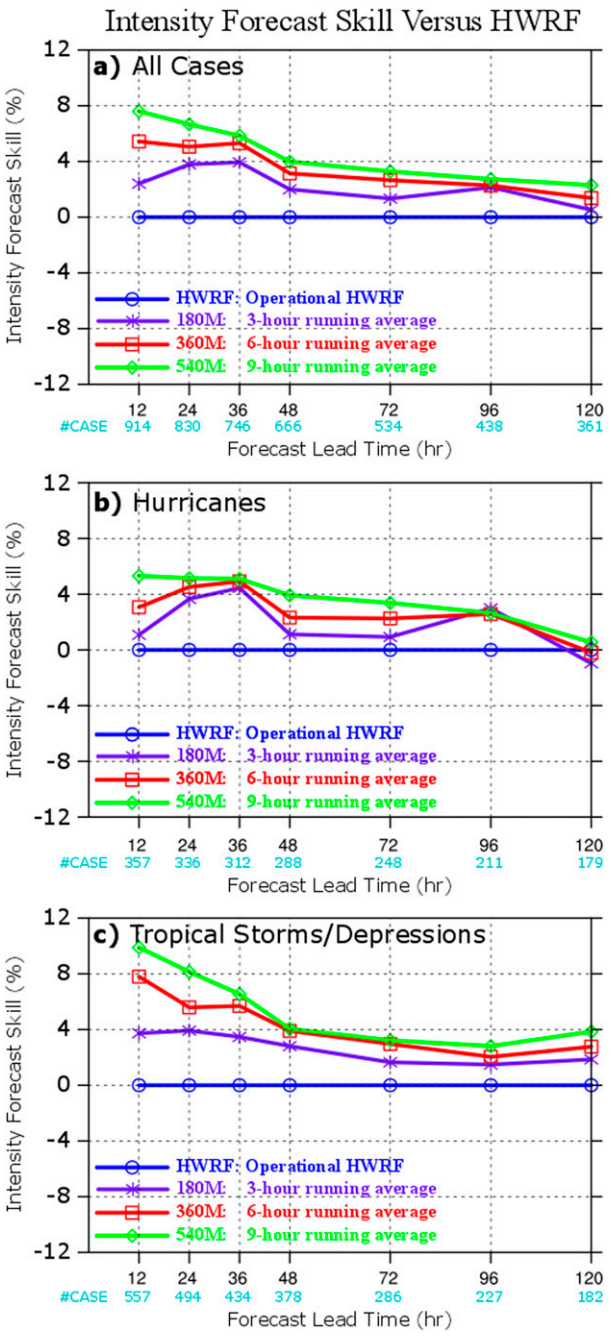

FIG. 13. Intensity forecast skill scores for (a) all forecast cycles, (b) forecast cycles with TCs of at least hurricane strength (≥64 kt) at the initial time, and (c) forecast cycles with TCs below hurricane strength at the initial time. In each panel, four forecasts are compared: the operational HWRF (HWRF; blue circles), the running mean of the HTCF tracker over a ±1.5-h time window (180M; purple asterisks), the running mean of the HTCF tracker over a ±3-h time window (360M; red squares), and the running mean of the HTCF tracker over a ±4.5-h time window (540M; green diamonds).

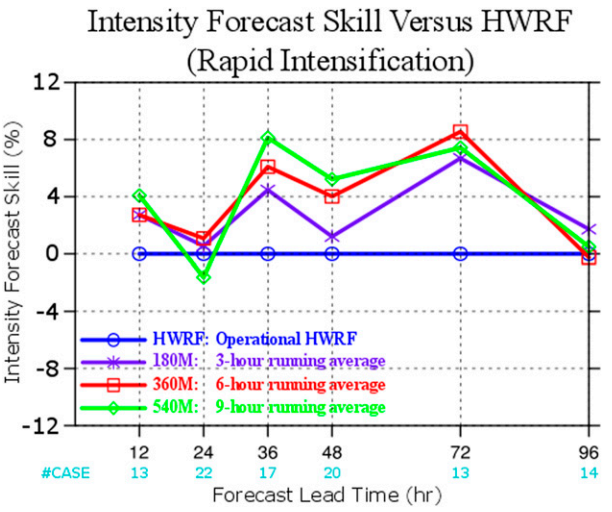

FIG. 14. Intensity forecast skill scores for forecast cycles in which rapid intensification (RI) occurred are compared for the operational HWRF (HWRF; blue circles), the running mean of the HTCF tracker over a ±1.5-h time window (180M; purple asterisks), the running mean of the HTCF tracker over a ±3-h time window (360M; red squares), and the running mean of the HTCF tracker over a ±4.5-h time window (540M; green diamonds).

seasons. Evidence was provided to show that temporal variations exist in both the TC track and intensity forecasts in the HWRF high-frequency outputs. These high-frequency outputs differed from the instantaneous operational 6-h HWRF forecasts produced by the GFDL tracker that were provided to the operational TC forecast centers and exhibited characteristics that were more consistent with BEST. Running means at various time windows were applied to the high-frequency outputs to study their statistical characteristics in comparison with the conventional 6-h outputs. The high-frequency data showed that predicted TC tracks exhibited small-scale oscillations with rotational periods from ~80 to ~100 min in Hurricanes Michael and Florence. Average amplitudes of TC track oscillations ranged from ~6 to ~8 km, while the deviations varied from ~2.5 to ~7 km, depending on the TC intensity. More intense TCs were associated with smaller track oscillations. An individual track fluctuation could be as large as 12 km, as shown in Hurricane Florence. An interesting result was that the high-frequency track fluctuations in HWRF forecasts resembled trochoidal motions as documented in theory and observations, such that these forecasts could be used to investigate detailed characteristics of TC trochoidal motions in future research.

The HTCF Pmin-based tracker data were used to estimate high-frequency track and Vmax fluctuations that were considered to be uncertainties in the 6-hourly GFDL tracker output. It was found that the variations in high-frequency track outputs had negligible impact on the track forecast verification when compared with BEST. On the other hand, the high-frequency fluctuations of Vmax could cause higher errors than 6-hourly instantaneous intensity forecasts. Running means were applied to the high-frequency HTCF data using centered windows of 3–9 h,

Brought to you by NOAA Central Library | Unauthenticated | Downloaded 09/30/21 02:54 PM UTC

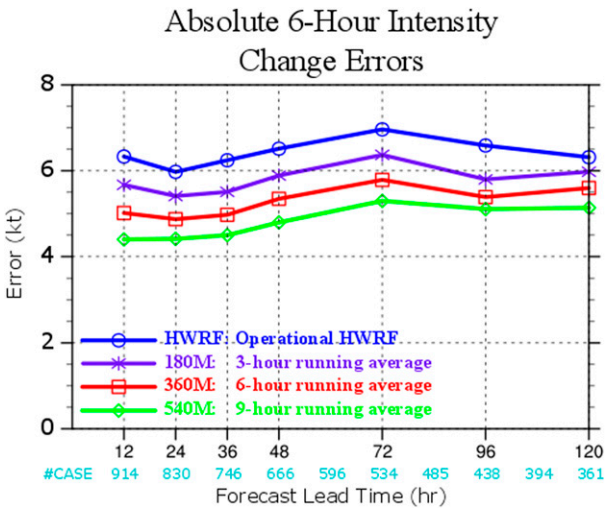

FIG. 15. Six-hour intensity change errors (kt) are compared for the operational HWRF (HWRF; blue circles), the running mean of the HTCF tracker over a ±1.5-h time window (180M; purple asterisks), the running mean of the HTCF tracker over a ±3-h time window (360M; red squares), and the running mean of the HTCF tracker over a ±4.5-h time window (540M; green diamonds).

and, as a result, TC intensity forecasts improved by up to 8% over the operational 6-hourly HWRF forecasts. A histogram analysis of the TC intensity based on the 6-h running mean of the high-frequency HTCF data showed that the temporal fluctuations of Vmax varied with TC intensity. The Vmax fluctuations were largest for category-2 hurricanes and were smaller for tropical storms and major hurricanes (category 3 or greater).

The relationship between the forecasts of TC intensity changes and DMW variation were also evaluated using HTCF data. The high-frequency DMW showed similar small-scale oscillations as in the high-frequency TC track, except with relatively large temporal and spatial scales. Results also showed that the Vmax was generally located at the right side of the TC track, where the TC steering flow added to the symmetric tangential wind of the TC vortex typically resulted in stronger winds. The HWRF high-frequency output was able to produce the relationship between TC intensity change and DMW time change revealed by BEST for RI TCs, that is, a TC either maintained or shrunk its size while TC was intensifying, while it either remained constant or grew it size when TCs weakened.

The high-frequency output from HWRF demonstrated that the model was able to capture variations associated with the TC track, intensity, and structure that were comparable to observations. These data could further improve impact-based forecasts for downstream applications, such as storm surge and inundation models that could more accurately represent characteristics of landfalling TCs. Although intensity forecast errors from 6-h running mean of the HTCF tracker output (360M) were smaller than those of the instantaneous, conventional GFDL tracker output (HWRF), that did not necessarily indicate that instantaneous intensity predictions from the operational HWRF were inaccurate; it may indicate that instantaneous Vmax reported by the GFDL tracker was near the tail of the distribution and that

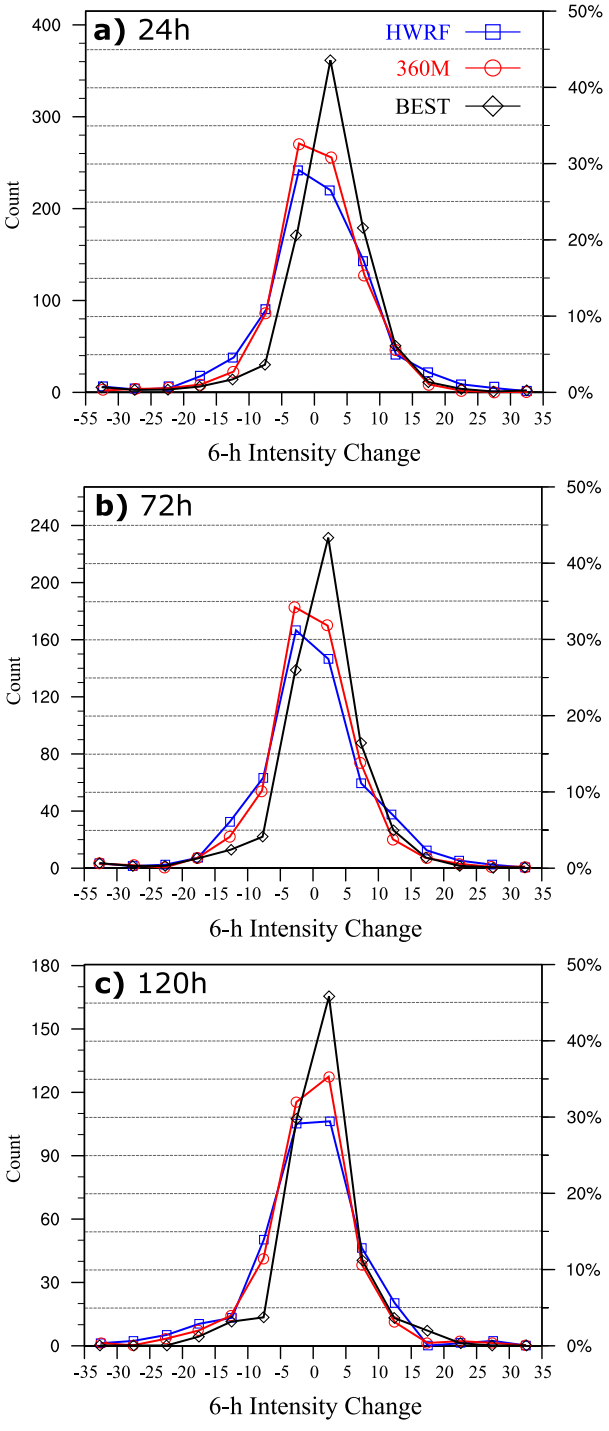

FIG. 16. Distributions of 6-h intensity change are compared for the operational HWRF (blue squares), running mean of the HTCF tracker over ±3-h time window (red circles), and BEST (black diamonds) at the following forecast lead times: (a) 24, (b) 72, and (c) 120 h. The count and percentage of the full sample for each bin are provided on the left *y* axis and right *y* axis, respectively.

Brought to you by NOAA Central Library | Unauthenticated | Downloaded 09/30/21 02:54 PM UTC

smoothing out that variability in high-frequency outputs was more consistent with BEST.

Future studies include examination of the impact of HCTF outputs on the interpolated or early model track and intensity forecasts, composition of high-frequency tracks based on TC track type, size, intensity to better understand trochoidal motions, and more in-depth analysis of the impact of HTCF data on coastal surge and inundation models.

Acknowledgments. The authors thank Dr. Lin Zhu at EMC for helping to conduct the intensity verification for RI cycles. This research was supported by NOAA's Hurricane Forecast Improvement Program. Author J. Zhang was supported by funding from NOAA Award NA19OAR0220186 and ONR Award N00014-20-1-2071.

Data availability statement. The dataset used in this study is the output from NOAA's operational hurricane forecast system, HWRF, and is available publicly. All analysis results can be reproduced using the method and parameters described in this paper.

REFERENCES

Aberson, S. D., J. A. Zhang, and K. N. Ocasio, 2017: An extreme event in the eyewall of Hurricane Felix on 2 September 2007. *Mon. Wea. Rev.*, **145**, 2083–2092, https://doi.org/10.1175/MWR-D-16-0364.1.

Bao, J.-W., S. G. Gopalakrishnan, S. A. Michelson, F. D. Marks, and M. T. Montgomery, 2012: Impact of physics representations in the HWRFX on simulated hurricane structure and wind–pressure relationships. *Mon. Wea. Rev.*, **140**, 3278–3299, https://doi.org/10.1175/MWR-D-11-00332.1.

Barnes, S. L., 1964: A technique for maximizing details in numerical weather map analysis. *J. Appl. Meteor.*, **3**, 396–409, https://doi.org/10.1175/1520-0450(1964)003<0396:ATFMDI>2.0.CO;2.

DeMaria, M., and J. L. Franklin, 2019: HFIP performance measures for rapid intensification. *2019 HFIP Annual Meeting*, Miami, FL, NOAA/NWS, 16 pp., https://hfip.org/sites/default/files/events/74/2-0900am-demaria.pdf.

Fischer, M. S., B. H. Tang, and K. L. Corbosiero, 2019: A climatological analysis of tropical cyclone rapid intensification in environments of upper-tropospheric troughs. *Mon. Wea. Rev.*, **147**, 3693–3719, https://doi.org/10.1175/MWR-D-19-0013.1.

Gopalakrishnan, S. G., F. D. Marks Jr., X. Zhang, J.-W. Bao, K.-S. Yeh, and R. Atlas, 2011: The experimental HWRF system: A study on the influence of horizontal resolution on the structure and intensity changes in tropical cyclones using an idealized framework. *Mon. Wea. Rev.*, **139**, 1762–1784, https://doi.org/10.1175/2010MWR3535.1.

——, S. B. Goldenberg, T. S. Quirino, X. Zhang, F. D. Marks Jr., K.-S. Yeh, R. Atlas, and V. Tallapragada, 2012: Toward improving high-resolution numerical hurricane forecasting: Influence of model horizontal grid resolution, initialization, and physics. *Wea. Forecasting*, **27**, 647–666, https://doi.org/10.1175/WAF-D-11-00055.1.

——, F. D. Marks Jr., J. A. Zhang, X. Zhang, J.-W. Bao, and V. Tallapragada, 2013: A study of the impacts of vertical diffusion on the structure and intensity of the tropical cyclones using the high resolution HWRF system. *J. Atmos. Sci.*, **70**, 524–541, https://doi.org/10.1175/JAS-D-11-0340.1.

Han, J., W. Wang, Y. C. Kwon, S. Hong, V. Tallapragada, and F. Yang, 2017: Updates in the NCEP GFS cumulus convection schemes with scale and aerosol awareness. *Wea. Forecasting*, **32**, 2005–2017, https://doi.org/10.1175/WAF-D-17-0046.1.

Harper, B. A., J. D. Kepert, and J. D. Ginger, 2010: Guidelines for converting between various wind averaging periods in tropical cyclone conditions. World Meteorological Organization TCP Sub-Project Rep. WMO/TD-1555, 54 pp.

Jordan, C. L., 1966: Surface pressure variations at coastal stations during the period of irregular motion of Hurricane Carla of 1961. *Mon. Wea. Rev.*, **94**, 454–458, https://doi.org/10.1175/1520-0493(1966)094<0454:SPVACS>2.3.CO;2.

Jordan, H. M., and D. J. Stowell, 1955: Some small-scale features of the track of Hurricane Ione. *Mon. Wea. Rev.*, **83**, 210–215, https://doi.org/10.1175/1520-0493(1955)083<0210:SSFOTT>2.0.CO;2.

Kaplan, J., and M. DeMaria, 2003: Large-scale characteristics of rapidly intensifying tropical cyclones in the North Atlantic basin. *Wea. Forecasting*, **18**, 1093–1108, https://doi.org/10.1175/1520-0434(2003)018<1093:LCORIT>2.0.CO;2.

——, ——, and J. Knaff, 2010: A revised tropical cyclone rapid intensification index for the Atlantic and eastern North Pacific basins. *Wea. Forecasting*, **25**, 220–241, https://doi.org/10.1175/2009WAF2222280.1.

Klotz, B. W., and D. S. Nolan, 2019: SFMR surface wind undersampling over the tropical cyclone life cycle. *Mon. Wea. Rev.*, **147**, 247–268, https://doi.org/10.1175/MWR-D-18-0296.1.

Landsea, C. W., and J. L. Franklin, 2013: Atlantic hurricane database uncertainty and presentation of a new database format. *Mon. Wea. Rev.*, **141**, 3576–3592, https://doi.org/10.1175/MWR-D-12-00254.1.

Lang, S. T. K., M. Leutbecher, and S. C. Jonesa, 2012: Impact of perturbation methods in the ECMWF ensemble prediction system on tropical cyclone forecasts. *Quart. J. Roy. Meteor. Soc.*, **138**, 2030–2046, https://doi.org/10.1002/qj.1942.

Lawrence, M. B., and B. M. Mayfield, 1977: Satellite observations of trochoidal motion of Hurricane Bell 1976. *Mon. Wea. Rev.*, **105**, 1458–1461, https://doi.org/10.1175/1520-0493(1977)105<1458:SOOTMD>2.0.CO;2.

Liu, Y., D.-L. Zhang, and M. K. Yau, 1999: A multiscale numerical study of Hurricane Andrew (1992). Part II: Kinematics and inner-core structures. *Mon. Wea. Rev.*, **127**, 2597–2616, https://doi.org/10.1175/1520-0493(1999)127<2597:AMNSOH>2.0.CO;2.

Marchok, T. P., 2002: How the NCEP tropical cyclone tracker works. *25th Conf. on Hurricanes and Tropical Meteorology*, San Diego, CA, Amer. Meteor. Soc., P1.13, https://ams.confex.com/ams/25HURR/techprogram/paper_37628.htm.

Marks, F. D., Jr., P. G. Black, M. T. Montgomery, and R. W. Burpee, 2008: Structure of the eye and eyewall of Hurricane Hugo (1989). *Mon. Wea. Rev.*, **136**, 1237–1259, https://doi.org/10.1175/2007MWR2073.1.

Mehra, A., V. Tallapragada, Z. Zhang, B. Liu, L. Zhu, W. Wang, and H. S. Kim, 2018: Advancing the state of the art in operational tropical cyclone forecasting at NCEP. *Trop. Cyclone Res. Rev.*, **7**, 51–56.

Miller, R. J., A. J. Schrader, C. R. Sampson, and T. L. Tsui, 1990: The automated tropical cyclone forecasting system (ATCF). *Wea. Forecasting*, **5**, 653–660, https://doi.org/10.1175/1520-0434(1990)005<0653:TATCFS>2.0.CO;2.

Nolan, D. S., and M. T. Montgomery, 2000: The algebraic growth of wavenumber one disturbances in hurricane-like vortices. *J. Atmos. Sci.*, **57**, 3514–3538, https://doi.org/10.1175/1520-0469(2000)057<3514:TAGOWO>2.0.CO;2.

Brought to you by NOAA Central Library | Unauthenticated | Downloaded 09/30/21 02:54 PM UTC

——, ——, and L. D. Grasso, 2001: The wavenumber-one instability and trochoidal motion of hurricane-like vortices. *J. Atmos. Sci.*, **58**, 3243–3270, https://doi.org/10.1175/1520-0469(2001)058,3243:TWOIAT.2.0.CO;2.

——, J. A. Zhang, and D. P. Stern, 2009: Evaluation of planetary boundary layer parameterizations in tropical cyclones by comparison of in situ observations and high-resolution simulations of Hurricane Isabel (2003). Part I: Initialization, maximum winds, and the outer-core boundary layer. *Mon. Wea. Rev.*, **137**, 3651–3674, https://doi.org/10.1175/2009MWR2785.1.

——, R. Atlas, K. T. Bhatia, and L. R. Bucci, 2013: Development and validation of a hurricane nature run using the joint OSSE nature run and the WRF Model. *J. Adv. Model. Earth Syst.*, **5**, 382–405, https://doi.org/10.1002/jame.20031.

——, J. A. Zhang, and E. W. Uhlhorn, 2014: On the limits of estimating the maximum wind speeds in hurricanes. *Mon. Wea. Rev.*, **142**, 2814–2837, https://doi.org/10.1175/MWR-D-13-00337.1.

OFCM, 2012: National Hurricane Operations Plan. U.S. Department of Commerce/National Oceanic and Atmospheric Administration Rep. FCM-P-2012, 168 pp.

Qin, N., D. L. Zhang, and Y. Lin, 2016: A statistical analysis of steady eyewall sizes associated with rapidly intensifying hurricanes. *Wea. Forecasting*, **31**, 737–742, https://doi.org/10.1175/WAF-D-16-0016.1.

Rogers, R., 2010: Convective-scale structure and evolution during a high-resolution simulation of tropical cyclone rapid intensification. *J. Atmos. Sci.*, **67**, 44–70, https://doi.org/10.1175/2009JAS3122.1.

Stern, D. P., J. L. Vigh, D. S. Nolan, and F. Zhang, 2015: Revisiting the relationship between eyewall contraction and intensification. *J. Atmos. Sci.*, **72**, 1283–1306, https://doi.org/10.1175/JAS-D-14-0261.1.

Tallapragada, V., C. Kieu, Y. Kwon, S. Trahan, Q. Liu, Z. Zhang, and I. H. Kwon, 2014: Evaluation of storm structure from the operational HWRF during 2012 implementation. *Mon. Wea. Rev.*, **142**, 4308–4325, https://doi.org/10.1175/MWR-D-13-00010.1.

Tong, M., S. Jason, V. Tallapragada, E. Liu, C. Kieu, and W. In-Hyuk Kwon, 2018: Impact of assimilating aircraft reconnaissance observations on tropical cyclone initialization and prediction using operational HWRF and GSI ensemble–variational hybrid data assimilation. *Mon. Wea. Rev.*, **146**, 4155–4177, https://doi.org/10.1175/MWR-D-17-0380.1.

Uhlhorn, E. W., and D. S. Nolan, 2012: Observational undersampling in tropical cyclones and implications for estimated intensity. *Mon. Wea. Rev.*, **140**, 825–840, https://doi.org/10.1175/MWR-D-11-00073.1.

Willoughby, H. E., 1990: Temporal changes of the primary circulation in tropical cyclone. *J. Atmos. Sci.*, **47**, 242–264, https://doi.org/10.1175/1520-0469(1990)047<0242:TCOTPC>2.0.CO;2.

——, and M. Chelmow, 1982: Objective determination of hurricane tracks from aircraft observations. *Mon. Wea. Rev.*, **110**, 1298–1305, https://doi.org/10.1175/1520-0493(1982)110<1298:ODOHTF>2.0.CO;2.

Yablonsky, R. M., I. Ginis, B. Thomas, V. Tallapragada, D. Sheinin, and L. Bernardet, 2015: Description and analysis of the ocean component of NOAA's operational Hurricane Weather Research and Forecasting (HWRF) Model. *J. Atmos. Oceanic Technol.*, **32**, 144–163, https://doi.org/10.1175/JTECH-D-14-00063.1.

Yang, H., L. Wu, and T. Xie, 2020: Comparisons of four methods for tropical cyclone center detection in a high-resolution simulation. *J. Meteor. Soc. Japan*, **98**, 379–393, https://doi.org/10.2151/jmsj.2020-020.

Yau, M. K., Y. Liu, and D.-L. Zhang, 2004: A multiscale numerical study of Hurricane Andrew (1992). Part VI: Small-scale inner-core structure and wind streaks. *Mon. Wea. Rev.*, **132**, 1410–1433, https://doi.org/10.1175/1520-0493(2004)132<1410:AMNSOH>2.0.CO;2.

Yeh, R. A., and V. Tallapragada, 2012: Toward improving high-resolution numerical hurricane forecasting: Influence of model horizontal grid resolution, initialization, and physics. *Wea. Forecasting*, **27**, 647–666, https://doi.org/10.1175/WAF-D-11-00055.1.

Zhang, J. A., and R. F. Rogers, 2019: Effects of parameterized boundary layer structure on hurricane rapid intensification in Shear. *Mon. Wea. Rev.*, **147**, 853–871, https://doi.org/10.1175/MWR-D-18-0010.1.

——, D. S. Nolan, R. F. Rogers, and V. Tallapragada, 2015: Evaluating the impact of improvements in the boundary layer parameterization on hurricane intensity and structure forecasts in HWRF. *Mon. Wea. Rev.*, **143**, 3136–3155, https://doi.org/10.1175/MWR-D-14-00339.1.

——, F. D. Marks Jr., J. A. Sippel, R. F. Rogers, X. Zhang, S. G. Gopalakrishnan, Z. Zhang, and V. Tallapragada, 2018: Evaluating the impact of improvement in the horizontal diffusion parameterization on hurricane prediction in the operational Hurricane Weather Research and Forecast (HWRF) Model. *Wea. Forecasting*, **33**, 317–329, https://doi.org/10.1175/WAF-D-17-0097.1.

Zhang, Z., 1997: Hurricane ensemble prediction using EOF-based perturbations. Ph.D. thesis, Florida State University, 174 pp.

——, and T. N. Krishnamurti, 1997: Ensemble forecasting of hurricane tracks. *Bull. Amer. Meteor. Soc.*, **78**, 2785–2795, https://doi.org/10.1175/1520-0477(1997)078<2785:EFOHT>2.0.CO;2.

——, and ——, 1999: A perturbation method for hurricane ensemble predictions. *Mon. Wea. Rev.*, **127**, 447–469, https://doi.org/10.1175/1520-0493(1999)127<0447:APMFHE>2.0.CO;2.

——, V. Tallapragada, C. Kieu, S. Trahan, and W. Wang, 2014: HWRF based ensemble prediction system using perturbations from GEFS and stochastic convective trigger function. *Trop. Cyclone Res. Rev.*, **3**, 145–161.

Brought to you by NOAA Central Library | Unauthenticated | Downloaded 09/30/21 02:54 PM UTC